JOURNAL OF AGRICULTURAL AND FOOD CHEMISTRY
ARTICLE

J. Agric. Food Chem. 2010, 58, 12357–12365 12357
DOI:10.1021/jf103762u

Photodegradation Pathways and Mechanisms of the Herbicide Metamifop in a Water/Acetonitrile Solution

Joon-Kwan Moon,[†] Jeong-Han Kim,[‡] and Takayuki Shibamoto*,[†]

[†]Department of Environmental Toxicology, University of California, Davis, California 95616, United States, and [‡]Department of Agricultural Biotechnology, College of Agriculture and Life Science, Seoul National University, Seoul 151-921, Korea

The herbicide metamifop and related compounds were irradiated by UV (λ = 300 nm) for various time periods, and degradation products were analyzed by gas chromatography and gas chromatography−mass spectrometry to assess the fate of metamifop in the environment. Nearly 10% of metamifop degraded within 30 min of irradiation and >80% degraded after 4 h. Among the metabolites, *N*-(2-fluorophenyl)-2-hydroxy-*N*-methylpropionamide (HPFMA) formed at the highest level (50.8%), followed by *N*-methyl-2-fluoroaniline (NMFA, 8.5%), *N*-methyl-2-oxo-*N*-phenylpropionamide (MOPPA, 6.6%), *N*-(2-fluorophenyl)-2-(4-hydroxyphenoxy)-*N*-methylpropionamide (HPPFMA, 3.9%), and 4-(6-chlorobenzooxazol-2-yloxy)phenol (CBOP, 1.2%) after 4 h of irradiation. HPPFMA degraded further to yield HPFMA (32.5%). CBOP also degraded to give 6-chloro-3*H*-benzooxazol-2-one (CBO, 6.6%). It is proposed that homolytic fission of C−O bonds occurred at the early stage of photolysis and further reactions with a hydroxyl radical and/or a hydrogen radical formed various metabolites. Standards, which are not commercially available, were synthesized in the authors' laboratory.

KEYWORDS: Metamifop; herbicide; photodegradation; UV irradiation

INTRODUCTION

Metamifop is a postemergent aryloxyphenoxypropionic acid herbicide (AOPP) used for the control of a wide range of annual and perennial grass weeds in cereal crops and rice. Postemergent herbicides are used to kill weeds after they have germinated. Metamifop is a relatively new herbicide developed in Korea (*1*) and is widely used to control weeds in many places, such as forest parks, golf courses, and gardens.

There is ongoing public concern about the increased use of pesticides due to their toxic and adverse effects on a number of nontarget species, including humans. Moreover, humans are unavoidably exposed to residual pesticides present in food and water. Many possible chronic effects of these pesticides have been reported, including carcinogenesis, neurotoxicity, and effects on reproduction (*2*). Even though tolerance levels of pesticide residues have been set by the U.S. Environmental Protection Agency (EPA), there are still many uncertain issues, such as whether the tolerance levels are absolutely safe, whether results from animal studies are completely applicable to human, and whether the actual amount of pesticide consumed by people is known. Several factors serve to reduce pesticide residues in food and the environment including sunlight, rain, and microbial activity. Hence, the fate of pesticides by photodegradation has been studied intensively over the past couple of decades (*2*).

Many pesticides and their metabolites have been found in environmental aqueous systems, such as groundwater, and their reaction pathways and mechanisms of photodegradation have been studied to assess their possible adverse effects on humans and ecosystems (*2*, *3*). Pesticides studied for photodegradation using simulated environmental aqueous systems include pirimicarb (*4*); carbetamide (*5*,*6*); phenmedipham (*7*); prometryn, terbutryn, simazine, and atrazine (*8*); and coumaphos and azinphos-methyl (*9*). However, new pesticides are continuously being developed and used, and there has not been sufficient research on the fates of new pesticides in the environment (*3*). Investigation of the pathways and mechanisms of photodegradation of newly developed pesticides is one avenue through which to obtain the knowledge useful for protecting humans and ecosystems from new toxic pollutants.

In the present study, metamifop and related compounds were UV-irradiated (λ = 300 nm) for various time periods, and degradation products were determined by gas chromatography (GC) and gas chromatography−mass spectrometry (GC-MS) to elucidate their photodegradation pathways and mechanisms.

MATERIALS AND METHODS

Chemicals and Reagents. Metamifop, 2-[4-(6-chlorobenzooxazol-2-yloxy)phenoxy]-*N*-(2-fluorophenyl)-*N*-methylpropionamide, was kindly donated by Dongbu Hannong Chemical Co. *N*-Methylaniline (NMA), 2-fluoroaniline, 2-benzoxazolinone, lithium hydroxide, 1,1′-carbonyldiimidazole, (*R*)-(+)-2-(4-hydroxyphenoxy)propionic acid (HPPA), iodomethane, 2 M oxalylchloride in dichloromethane, 2-amino-5-chlorophenol, thiophosgene, hydroquinone (HQ), pyruvic acid, *N*-methyl-*N*-(trimethylsilyl)trifluoroacetamide (MSTFA), and 2-chlorobenxazole were purchased from Sigma-Aldrich Corp. (St. Louis, MO). Ethyl acetate, dichloromethane, dimethylformamide (DMF), and hexane were purchased from Fisher Scientific Co. (Rochester, NY).

*Author to who correspondence should be addressed [phone (530) 752-4924; fax (530) 752-3394; e-mail tshibamoto@ucdavis.edu].

Published on Web 11/10/2010

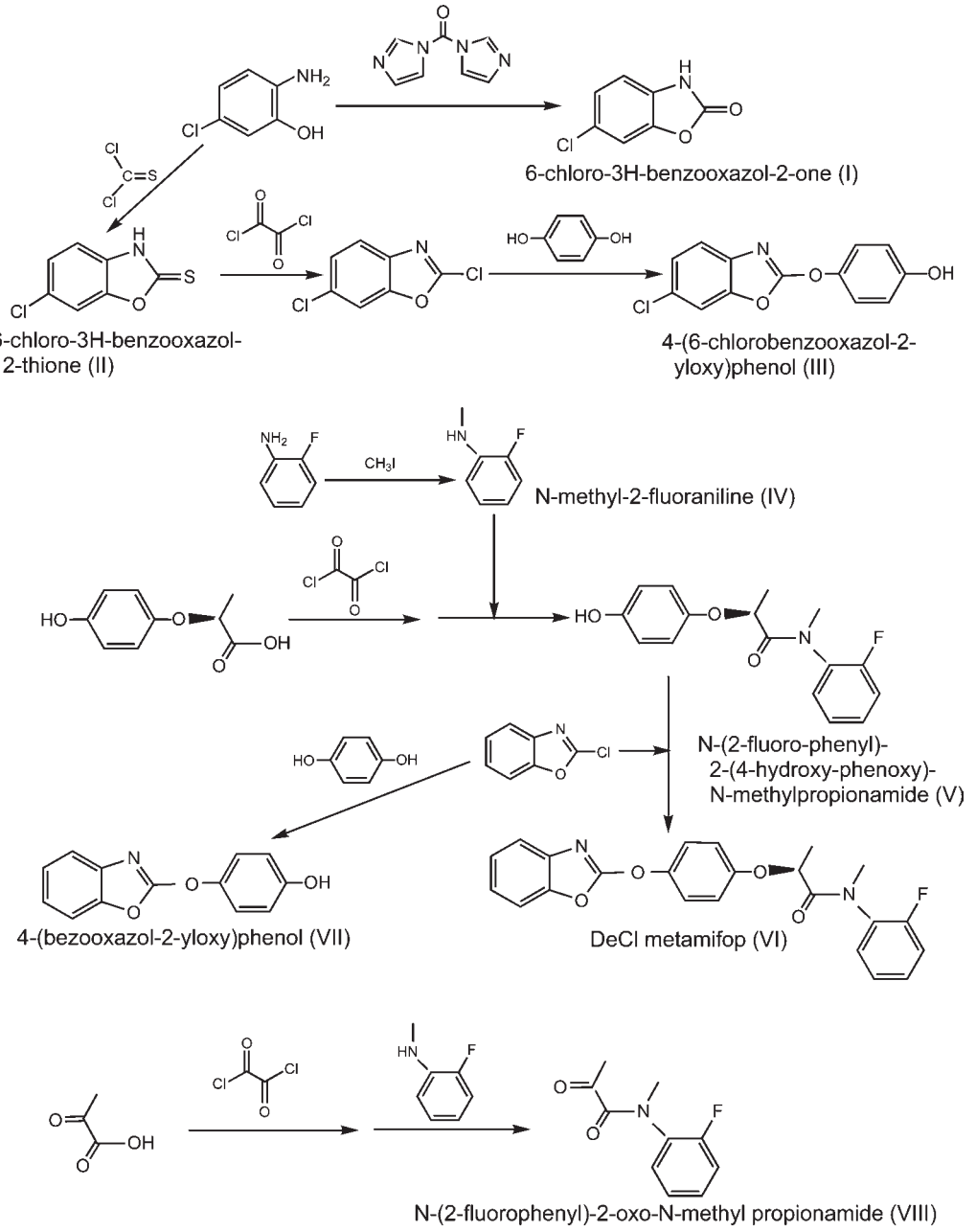

Figure 1. Overall reaction schemes for the authentic chemicals synthesized in the present study.

Synthesis of Authentic Chemicals. The authentic chemicals are not commercially available and were synthesized in our laboratory. The overall reaction schemes of the authentic chemicals synthesized in the present study are shown in **Figure 1** and their preparation procedures are as follows:

6-Chloro-3H-benzooxazol-2-one (*CBO, **I***). 1,1′-Carbonyldiimidazole (1.62 g) was added to a 20 mL DMF solution of 2-amino-5-chloropenole (1.43 g), and the solution was heated at 60 °C for 4 h. After cooling to room temperature, the reaction mixture was poured into 100 mL of water and then extracted twice with 100 mL of ethyl acetate. After removal of water with sodium sulfate, the solvent was removed using a rotary flash evaporator, and the residual material was purified by silica gel column chromatography. 6-Chloro-3*H*-benzooxazol-2-one was obtained as a white solid (1.47 g, yield = 87%).

6-Chloro-3H-benzoxazol-2-thione (***II***). Thiophosgene (520 mg) was added to a 10 mL dichloromethane solution of 2-amino-5-chlorophenol (710 mg), and the reaction solution was stirred for 30 min at room temperature. The reaction mixture was dissolved into 50 mL of water and then extracted twice using 100 mL of ethyl acetate. After the solvent had been removed with a rotary flash evaporator, the residual material was purified by silica gel column chromatography with ethyl acetate/hexane (1:3, v/v) as elution solvent. 6-Chloro-3*H*-benzooxazol-2-thione was obtained as a brown solid (620 mg, yield = 67%): $M^+ = 185$ (100), *m*/*z* 187 (37), 125 (24), 62 (10).

4-(6-Chlorobenzooxazol-2-yloxy)phenol (*CBOP, **III***). One milliliter of oxalyl chloride solution (2M) was added to a 20 mL ethyl acetate solution of 6-chloro-3*H*-benzooxazol-2-thione (600 mg), and then 10 μL of DMF was added. The mixture was stirred for 8 h at room temperature, and subsequently the solvent was removed from the reaction mixture using a rotary flash evaporator. After the residual material had been dissolved into 25 mL of ethyl acetate, 500 mg each of HQ and potassium carbonate was added, followed by 20 mL of water. The reaction solution was stirred for 4 h. After the organic layer had been dried over anhydrous sodium sulfate, the solvent was removed with a rotary flash evaporator. The residual material was purified by silica gel column chromatography with ethyl acetate/hexane (1:2, v/v) as an elution solvent. 4-(6-Chlorobenzooxazol-2-yloxy)phenol was obtained as pale brown solid (250 mg, yield = 29%).

N-Methyl-2-fluoroaniline (*NMFA, **IV***). Iodomethane (1.4 g) was added to a 20 mL DMF solution of 2-fluoroaniline (1.15 g) containing

Table 1. Structures, Names, and Abbreviations of the Chemicals Discussed in the Present Study along with Their Mass Spectra

Structure	Full Name	Abbreviation	GC-MS Spectrum
	N-methyl-2-fluoroaniline	NMFA	125 (82, M^+), 124(10), 83(13), 77(38)
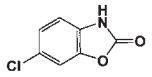	6-Chloro-3H-benzooxazol-2-one	CBO	171 (33), 169 (100, M^+), 125 (13), 113(35), 78 (41)
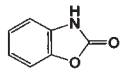	3H-Benzooxazol-2-one	BO	135 (100, M^+), 91 (18), 79 (59), 64 (13), 52 (44)
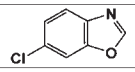	6-Chloro-benzooxazole	6-CB	155 (3), 153 (100, M^-), 127 (15), 125 (54), 98 (11), 90 (9), 63 (59)
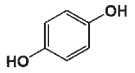	Hydroquinone	HQ	110 (100, M^+), 81 (32), 55 (17), 53 (24)
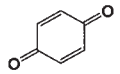	[1,4]Benzoquinone	BQ	108 (88, M+), 82 (36), 80 (22), 54 (100), 52 (20)
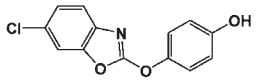	4-(6-Chloro-benzooxazol-2-yloxy)-phenol	CBOP	263 (34), 261 (100, M^+), 182(29), 170 (14), 121 (7.8), 65 (21)
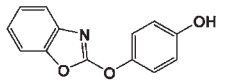	4-(Benzooxazol-2-yloxy)-phenol	BOP	227(100, M^+), 182(15), 170 (14), 154(33), 106(12), 65(26)
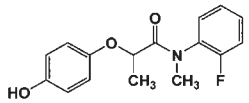	N-(2-Fluoro-phenyl)-2-(4-hydroxy-phenoxy)-N-methyl-propionamide	HPPFMA	289(11, M^+), 288 (60), 207 (11), 180 (100), 152 (85), 137(9), 125 (24), 124(38), 123(45), 119 (14), 91 (15), 77 (24)
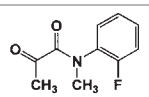	N-(2-Fluoro-phenyl)-N-methyl-2-oxo-propionamide	FPMOPA	195(24, M^+), 152(97), 137(17), 124(100), 109(12), 95(15), 77 (34)
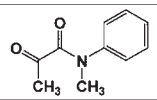	N-Methyl-2-oxo-N-phenyl-propionamide	MOPPA	177 (13, M^+), 149 (9), 134 (100), 106 (85), 77 (45), 51 (19)
	N-Methyl aniline	NMA	107 (95), 106 (100, M^+), 86 (34), 77 (11), 51 (24)
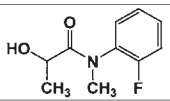	N-(2-Fluoro-phenyl)-2-hydroxy-N-methyl-propionamide	HPFMA	197 (9, M^+), 182 (3), 153 (39), 125 (78), 124 (100), 109 (6), 95 (13), 77 (32)
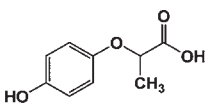	R-(+)-2-(4-hydroxyphenoxy)propionic acid	HPPA	Di-silylated; 326 (83, M^+), 311 (8), 265 (16), 239 (6), 209 (38), 181 (72), 165 (16), 112 (13), 73 (100)
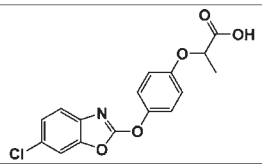	2-[4-(6-Chloro-benzooxazol-2-yloxy)-phenoxy]-propionic acid	Fenoxaprop	Mono-silylated; 407 (33), 405 (78, M^+), 348 (20), 346 (54), 290 (29), 288 (82), 263 (9), 261 (27), 159 (13), 73 (100)
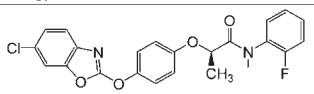	2-[4-(6-Chloro-benzooxazol-2-yloxy)-phenoxy]-N-(2-fluoro-phenyl)-N-methyl-propionamide	Metamifop	442 (21), 440 (58, M^+), 290 (23), 288 (64), 180 (100), 152 (83), 123 (28), 77 (20)
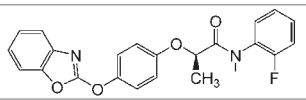	2-[4-(Benzooxazol-2-yloxy)-phenoxy]-N-(2-fluoro-phenyl)-N-methyl-propionamide	DeCl	406 (100, M^-), 254(86), 227(13), 210 (7), 180(81), 152(67), 137(8), 123(26), 122(33), 91 (8), 77 (14)

40 mg of sodium hydride dispersed in 60% mineral oil and stirred for 6 h at room temperature. Ethyl acetate (50 mL) was added to the reaction mixture, and the solution was washed twice with 50 mL of water. After the organic layer had been dried over anhydrous sodium sulfate, the solvent

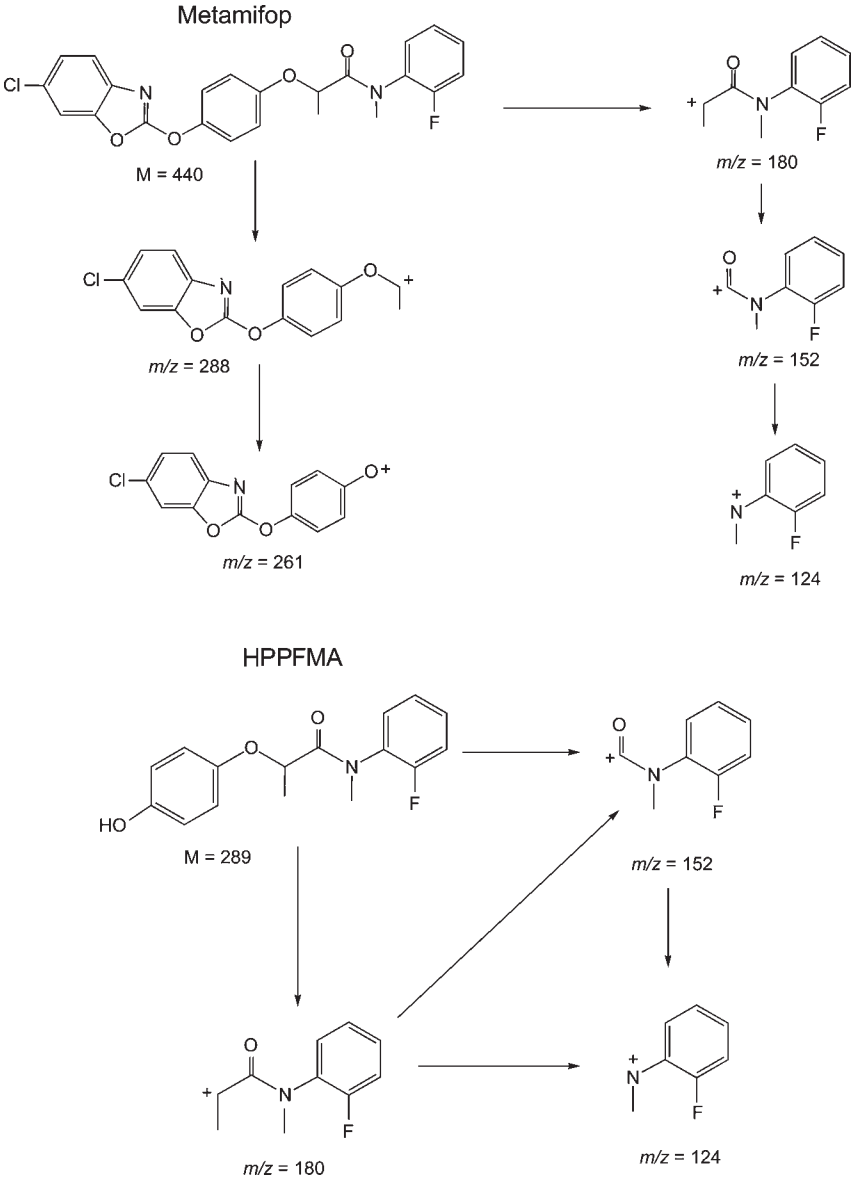

Figure 2. Proposed mass spectral fragmentations of two typical compounds, metamifop and HPPFMA.

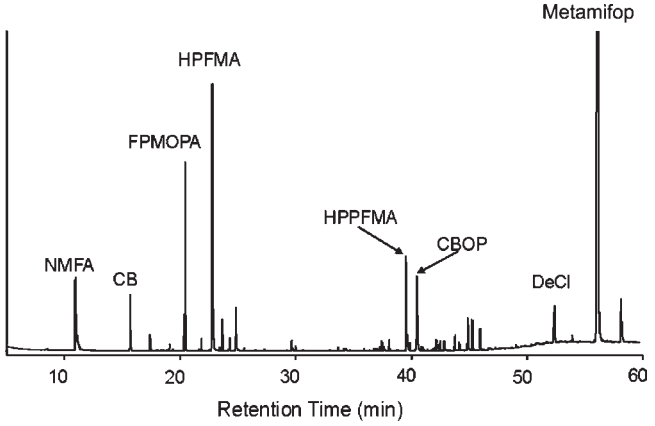

Figure 3. Typical gas chromatogram of a metamifop irradiated sample.

was removed with a rotary flash evaporator. The residual material was purified with silica gel column chromatography with ethyl acetate/hexane (1:5, v/v) as elution solvent. *N*-Methyl-2-fluoroaniline was obtained as a yellow oil (753 mg, yield = 61%): $M^+ = 125$ (100), *m*/*z* 124 (10), 83 (13), 77 (38).

N-(2-Fluorophenyl)-2-(4-hydroxyphenoxy)-N-methylpropionamide (*HPPFMA, V*). A dichloromethane solution (3 mL) of oxalylchloride (2 M) containing 2 drops of DMF was added to a 100 mL ethyl acetate solution of HPPA (900 mg) in an ice bath, and the solution was stirred for 1 h at room temperature. After the reaction, the solvent was removed by a rotary flash evaporator under reduced pressure. The residual material was redissolved into 100 mL of ethyl acetate. To this solution were added 1.2 g of *N*-methyl-2-fluoroanile and 50 mL of 1 M sodium bicarbonate solution followed by 1 h of stirring in an ice bath. The organic layer was collected from the reaction mixture and dried over anhydrous sodium sulfate. After the solvent had been removed by rotary flash evaporator under reduced pressure, the residual material was purified by silica gel column chromatography with ethyl acetate/hexane (1:2, v/v) as elution solvent. *N*-(2-Fluorophenyl)-2-(4-hydroxyphenoxy)-*N*-methylpropionamide was obtained as a white solid (770 mg, yield = 54%).

2-[4-(Benzooxazol-2-yloxy)phenoxy]-N-(2-fluorophenyl)-N-methylpropionamide (*DeCl Metamifop, VI*). 2-Chlorobenoxazole (153 mg) was added dropwise to a 100 mL DMF solution of HPPFMPA (290 mg) containing 140 mg of potassium carbonate. After the mixture had been stirred for 6 h at room temperature, the reaction mixture was transferred to a 125 mL separatory funnel and 20 mL of water was added. The reaction mixture was extracted twice with 50 mL of ethyl acetate. After the extract had been dried over anhydrous sodium sulfate, the solvent was removed by a rotary flash evaporator under reduced pressure. The residual material

was purified by silica gel column chromatography with ethyl acetate/hexane (1:3, v/v) as elution solvent. DeCl metamifop was obtained as a white solid (385 mg, yield = 95%).

4-(Benzooxazol-2-yloxy)phenol (*BOP*, ***VII***). 2-Chlorobenooxazole (153 mg) was added dropwise to a 10 mL DMF solution of hydroquinone (110 mg) containing 140 mg of potassium carbonate. After the solution had been stirred for 6 h at room temperature, the reaction mixture was transferred to a 125 mL separatory funnel and 20 mL of water was added. The reaction mixture was extracted twice with 50 mL of ethyl acetate. After the extract had been dried over anhydrous sodium sulfate, the solvent was removed by a rotary flash evaporator. The residual material was purified by silica gel column chromatography with ethyl acetate/hexane (1:3, v/v) as elution solvent. 4-(Benzooxazol-2-yloxy)phenol was obtained as white solid (135 mg, yield = 67%): $M^+ = 227$ (100), *m*/*z* 182 (15), 170 14), 154 (33), 106 (12), 65 (26).

N-(2-Fluorophenyl)-2-oxo-N-methylpropionamide (*FPMOPA*, ***VIII***). A 3 mL dichloromethane solution of 2 M oxalylchloride containing 2 drops of DMF was added to a 50 mL ethyl acetate solution of pyruvic acid (270 mg) and stirred for 1 h at room temperature in an ice bath. After the solvent had been removed from the reaction mixture, the residual material was redissolved into 50 mL of ethyl acetate. To this solution was added 30 mL of a 1 M sodium bicarbonate solution containing 400 mg of *N*-methyl-2-fluoroaniline in an ice bath. After the organic layer had been

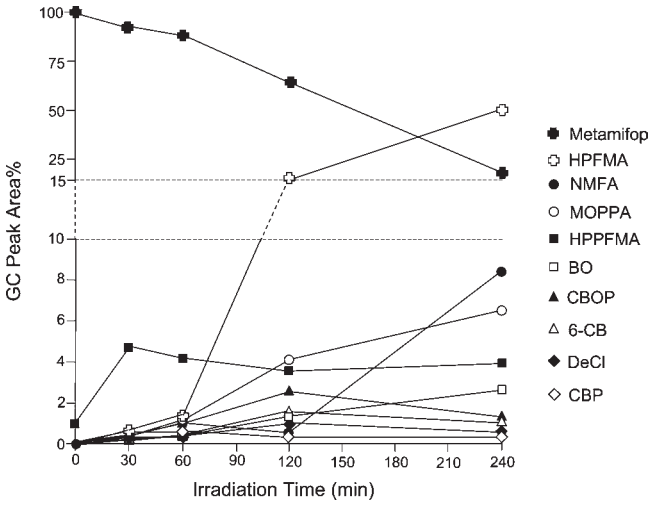

Figure 4. Kinetics of metamifop photolysis.

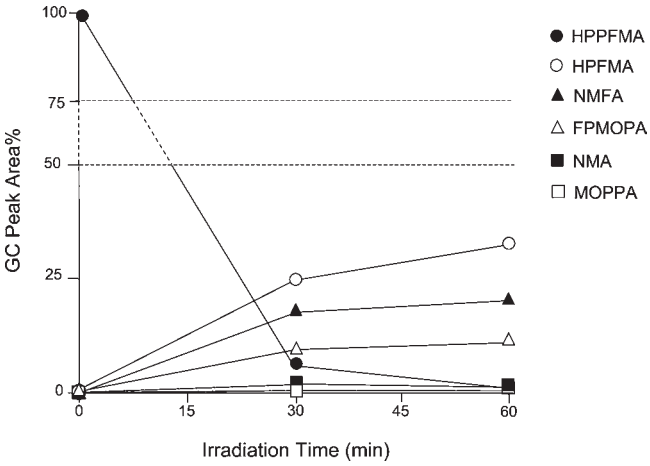

Figure 6. Kinetics of HPPFMA photolysis.

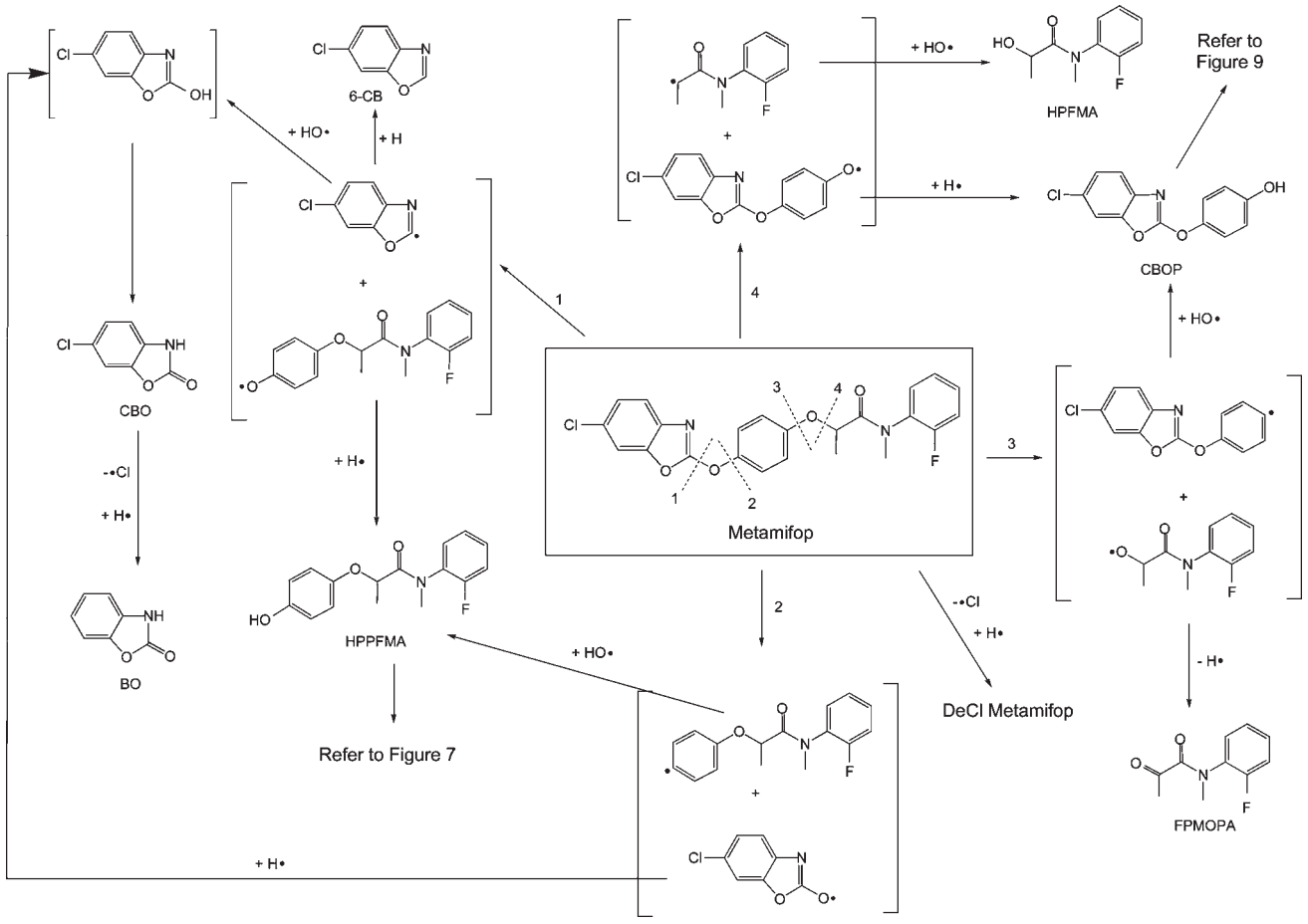

Figure 5. Proposed photodegradation pathways of metamifop.

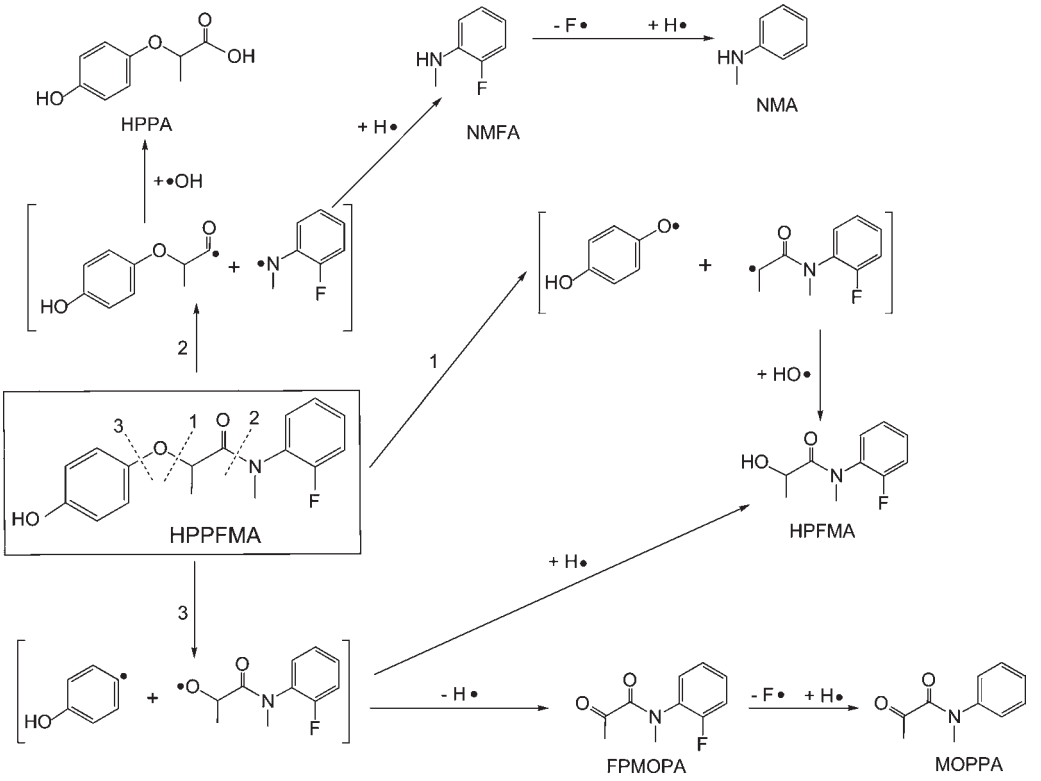

Figure 7. Proposed photodegradation pathways of HPPFMA.

dried over anhydrous sodium sulfate, the solvent was removed by a rotary flash evaporator. The residual material was purified by silica gel column chromatography with ethyl acetate/hexane (1:2, v/v) as elution solvent. *N*-(2-Fluorophenyl)-2-oxo-*N*-methylpropionamide was obtained as a colorless oil (209 mg, yield = 35%): M^+ = 195 (24), *m*/*z* 152 (97), 137 (17), 124 (100), 109 (12), 95 (15), 77 (34).

Photoirradiation and Preparation of Irradiated Samples for Analysis. A 50% aqueous acetonitrile solution (10 mL) of each chemical (10 mg of metamifop, 5 mg each of CBO, CBOP, HPPFMA, or HPFMA) was irradiated in a quartz test tube (13 mm × 120 mm) for various time periods with a model RPR-100 Rayonet Photochemical Reactor equipped with RPR 3000A UV lamps (λ_{max} = 300 nm) and sample carousel (Southern New England UV Co., Branford, CT).

The irradiated sample solution (0.5 mL) was added to a 3 mL aqueous sodium chloride solution (15%) and then extracted twice with 5 mL of dichloromethane. After the extract had been dried over anhydrous sodium sulfate, the solvent was removed with a purified nitrogen stream. The residual material was dissolved in 200 μL of dichloromethane and stored at 5 °C until analysis.

GC-MS Analysis of Photodegradation Products. Chemicals in the dichloromethane solution were identified by comparison with the Kovats GC retention index *I* and by the mass spectral fragmentation pattern of each component compared with those of authentic compounds.

An Agilent model 6890 GC interfaced to an Agilent 9571A mass selective detector (GC-MS) and equipped with a 30 m × 0.25 mm i.d. (d_f = 0.5 μm) DB-5 bonded-phase fused silica capillary column (Agilent, Folsom, CA) was used for mass spectral identification of the GC components at a MS ionization voltage of 70 eV. The helium carrier gas flow rate was 1.0 mL/min at a splitless injection. The injector and detector temperatures were 260 and 280 °C, respectively. The oven temperature was held at 50 °C and then programmed to increase to 290 at 5 °C/min and held for 20 min.

Identification of HPPA and Fenoxaprop in a Metamifop Irradiated Sample by GC-MS after Trimethylsilylation. After the irradiated sample (200 μL) of metamifop had been freeze-dried, 200 μL of MSTFA was added and then heated at 70 °C for 1 h. The reaction mixture was condensed with a purified nitrogen stream. The residual material was redissolved into 200 μL of dichloromethane and subjected to GC-MS.

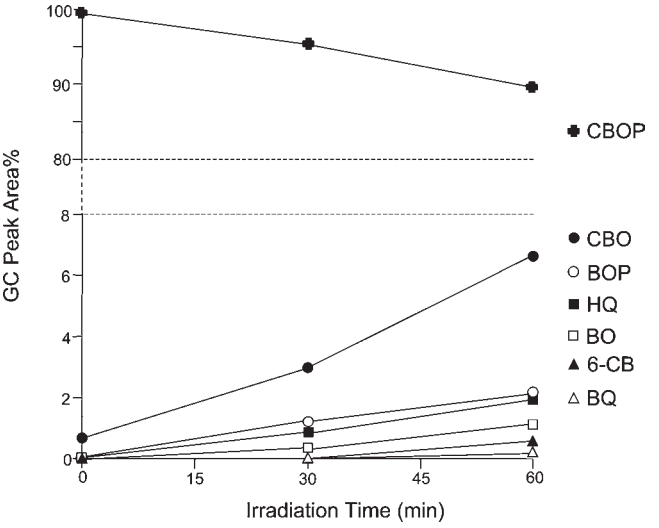

Figure 8. Kinetics of CBOP photolysis.

RESULTS AND DISCUSSION

Table 1 shows the structures, names, and abbreviations of the chemicals discussed in the present study along with their mass spectra. Mass fragmentation patterns of these compounds were relatively simple because of the presence of unsaturated rings. Proposed mass spectral fragmentations of two typical compounds are shown in **Figure 2**.

Figure 3 shows a typical gas chromatogram of a metamifop irradiated sample. **Figure 4** shows the kinetics of metamifop photolysis. Nearly 10% of metamifop degraded within 30 min of irradiation and >80% degraded after 4 h. HPFMA formed predominantly (50.8%), followed by NMFA (8.5%), MOPPA (6.6%), and HPPFMA (3.9%) after 4 h of irradiation. Other photodegradation products formed at levels of 1−2%. It is

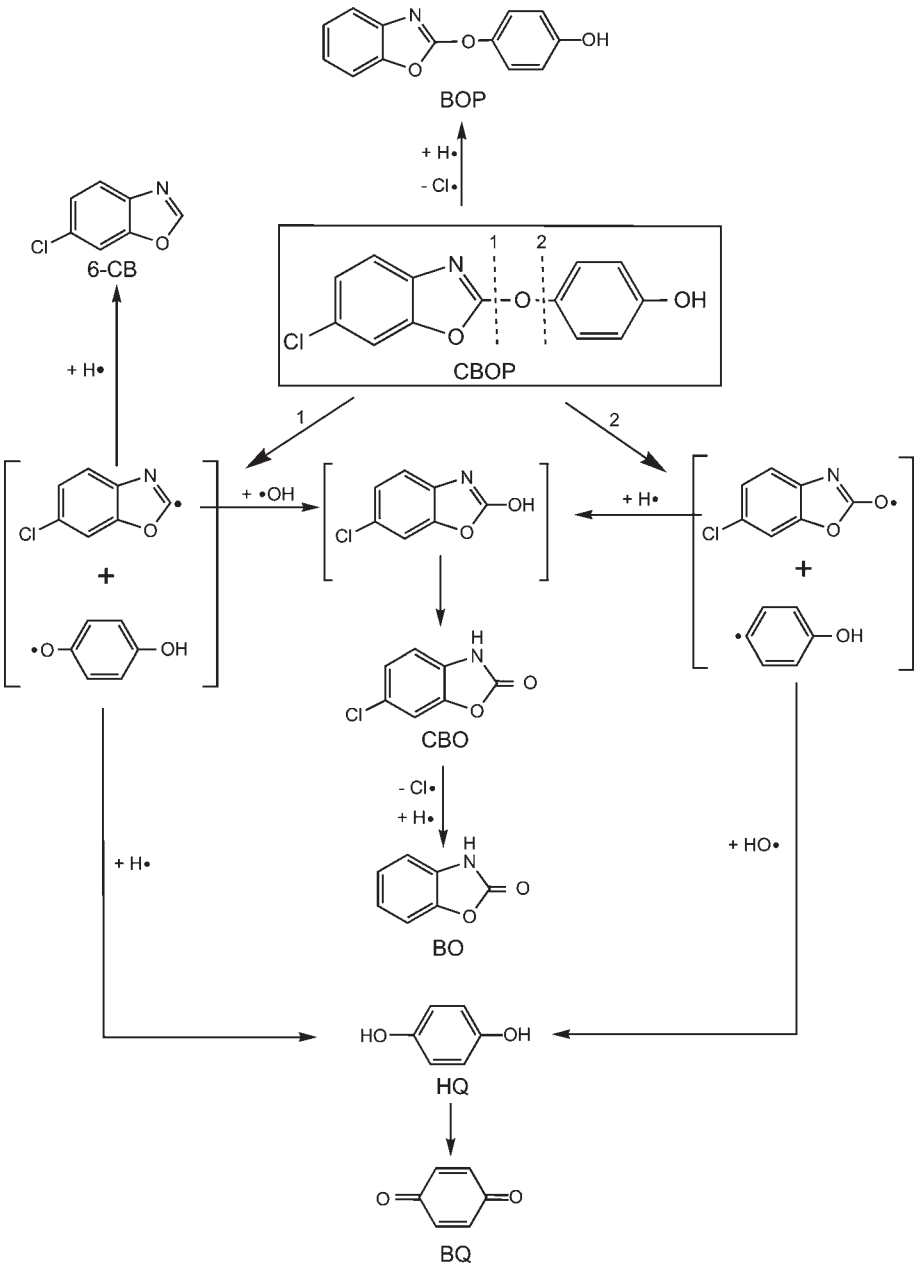

Figure 9. Proposed photodegradation pathways of CBOP.

interesting that HPPFMA formed the highest level (4.7%) after 30 min of irradiation, whereas HPFMA formed only 0.9% in same period of time.

Figure 5 shows the proposed photodegradation pathways of metamifop. The occurrence of homolytic fission of C−O bonds (processes 1−4) at the early stage of photodegradation is proposed. Radical species •H, •OH, and •Cl may be formed from metamifop or water at the early stage of photoirradiation and then subsequently react with other radicals from metamifop to give the photodegradation products. Also, dechlorination of metamifop to yield DeCl metamifop occurred. Many studies have reported the formation of •OH in various aqueous solutions of organic pollutants (*10*, *11*), including pesticides (*12*−*14*). Also, formation of radical intermediates, including •H, in the photodecomposition of water has previously been reported (*15*). On the basis of these studies and the results of the present study, the pathways in **Figure 5** were hypothesized.

Figure 6 shows the kinetics of HPPFMA photolysis. Photodegradation of HPPFMA occurred relatively quickly. It degraded by >90% within 30 min of irradiation. After 60 min of irradiation, about 0.7% remained. Therefore, relatively high

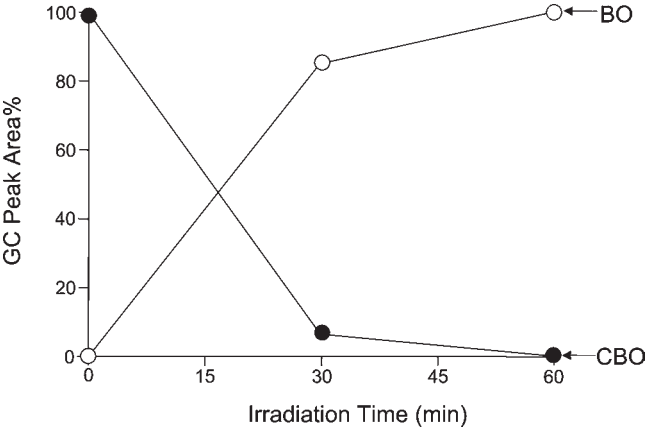

Figure 10. Kinetics of CBO photolysis.

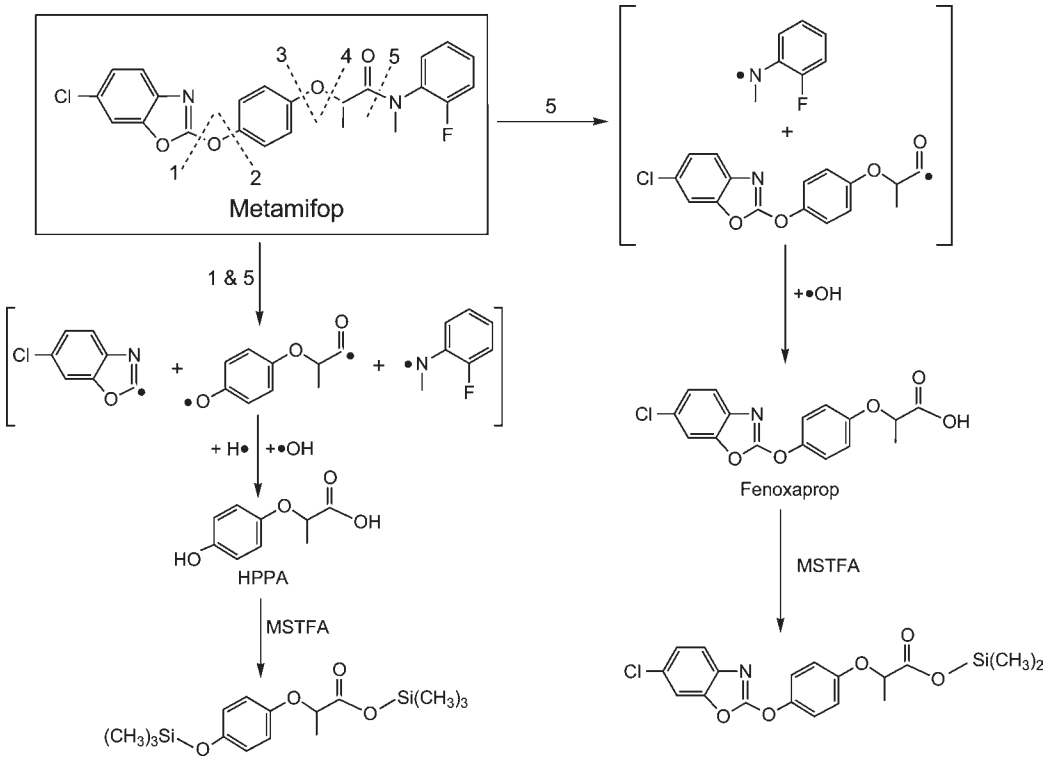

Figure 11. Proposed formation pathways of silylated HPPA and fenoxaprop from metamifop.

levels of photodegradation products were recovered. Among the photodegradation products, HPFMA formed in the greatest amount after 60 min of irradiation (GC peak area % = 32.5), followed by NFMA (19.3%), FPMOPA (10.3%), and NMA (1.3%).

Figure 7 shows the proposed photodegradation pathways of HPPFMA. As this figure shows, HPPFMA degraded to form HPFMA. HPFMA must be relatively resistant to photodegradation because no degradation products were detected in this HPPFMA solution. Moreover, photodegradation did not occur when HPFMA itself was irradiated by a UV light in an aqueous acetonitrile solution. Formation of NMFA, followed by cleavage of the C−N bond in HPPFMA upon irradiation (process 2), was observed in the present study. Formation of amines after cleavage of the C−N bond in triazine herbicides upon photodegradation has been reported previously (*16*).

Figure 8 shows the kinetics of CBOP photolysis. Only about 10% of CBOP was degraded upon 60 min of irradiation under the conditions used in the present study. Among the photodegradation products, CBO formed in the greatest amount after 60 min of irradiation (GC peak area % = 6.6), followed by BOP (2.2%) and HQ (1.9%).

Figure 9 shows the proposed photodegradation pathways of CBOP. It is proposed that homolytic fission occurred at the ether bonds of CBOP to form the radicals as shown in **Figures 5** and **7**. CBOP exhibited the same pattern in metamifop photolysis as did HPPFMA. The amount of CBOP formed was greatest at 2 h of irradiation and declined thereafter, indicating that further photodegradation occurred on CBOP after it formed from metamifop.

When CBO was irradiated, complete dechlorination resulted giving, BO (3*H*-benzooxazol-2-one) after 60 min of irradiation (**Figure 10**). No other photodegradation products were observed under the conditions used in the present study. Dechlorination was also observed in the herbicide oxyfluofen upon irradiation under sunlight in an aqueous solution (*17*).

It has been reported that when the pesticide ethiofencarb was degraded by an Oriel solar simulation unit in an organic solution (*18*), ethiofencarb phenol was formed via homolytic fission of an ether bond by mechanisms similar to those shown in **Figures 4**, **6**, and **8** (*19*). Formation of a phenolic radical followed by absorption of a hydrogen radical to yield phenols, including hydroquinone in the case of the present study, seems to be a common pathway in pesticides containing a phenolic moiety such as fenazaquin (*20*) and dichlorprop (*21*). Dechlorination from CBOP to BOP as well as from CBO to BO occurred.

It was difficult to detect the presence of HPPA and fenoxaprop by GC-MS in the metamifop irradiated sample due to their low volatility. However, trimethylsilylation allowed these compounds to be detected. **Figure 11** shows the proposed formation pathways of these two photodegradation products.

The herbicidal activity of metamifop and fenoxaprop, which are newly identified photodegradation product of metamifop, has been well established (*1*). They inhibit the action of acetyl-CoA carboxylase. The results obtained in the present study demonstrate that metamifop degrades readily upon UV irradiation with homolytic fission of the C−O bond as a first step of the degradation pathway. Further degradations of its photodegradation products, CBOP and HPPFMA, were also observed. Many photodegradation products found in the present study contained more water-soluble moieties such as hydroxyl, acid, and dicarbonyl groups, suggesting that metamifop enters aqueous systems upon photolysis. Although it is difficult to simulate what happens in the natural environment, a study using a model system is one avenue to assess the fate of pesticides in the environment.

LITERATURE CITED

(1) Moon, J.-K.; Keum, Y.-S.; Hwang, E.-C.; Park, B.-S.; Chang, H.-R.; Li, Q. X.; Kim, J.-H. Hapten synthesis and antibody generation for a new herbicide, metamifop. *J. Agric. Food Chem.* **2007**, *55*, 5416−5422.

(2) Burrows, H. D.; Canle, L. M.; Santaballa, J. A.; Steenken, S. Reaction pathways and mechanisms of photodegradation of pesticides. *J. Photochem. Photobiol. B: Biol.* **2002**, *67*, 71−108.
(3) Foster, S. S. D.; Chilton, P. J.; Stuart, M. E. Mechanisms of groundwater pollution by pesticides. *J. Inst. Water Environ. Manag.* **1991**, *5*, 186−193.
(4) Pirisi, F. M.; Cabras, P.; Garau, V. L.; Melis, M.; Secchi, E. Photodegradation of pesticides. Photolysis rates, and half-life of pirimicarb and its metabolites in reactions in water and in solid phase. *J. Agric. Food Chem.* **1996**, *44*, 2417−2422.
(5) Meallier, P.; Mamouni, A.; Mansour, M. Photodegradation of pesticides − VII. Photodegradation of carbetamide − photoproducts. *Chemosphere* **1993**, *26*, 1917−1923.
(6) Percherancier, J. P.; Chapelon, R.; Pouyet, B. Semiconductor-sensitized photodegradation of pesticides in water: the case of carbetamide. *J. Photochem. Photobiol. A: Chem.* **1995**, *87*, 261−266.
(7) Guittonneau, S.; Khelifi, F.; Meallier, P. Photodegradtion of pesticides on adsorbed phases: photodegradation of phenmedipham. *Environ. Technol.* **1995**, *16*, 477−482.
(8) Kiss, A.; Rapi, S.; Csutras, C. GC/MS studies on revealing products and reaction mechanism of photodegradation of pesticides. *Microchem. J.* **2007**, *85*, 13−20.
(9) Franko, M.; Sarakha, M.; Cibej, A.; Boskin, A.; Bavcon, M.; Trebse, P. Photodegradation of pesticides and application of bioanalytical methods for their detection. *Pure Appl. Chem.* **2005**, *77*, 1727−1736.
(10) Kochany, J.; Bolton, J. R. Mechanism of photodegradation of aqueous organic pollutants. 1. EPR spin-trapping technique for the determination of $^{\bullet}OH$ radical rate constants in the photooxidation of chlorophenols following the photolysis of H_2O_2. *J. Phys. Chem.* **1991**, *95*, 5116−5120.
(11) Sundstrom, D. W.; Weir, B. A.; Klei, H. E. Destruction of aromatic pollutants by UV light catalyzed oxidation with hydrogen peroxide. *Environ. Prog.* **1989**, *8*, 6−9.
(12) Wu, C.; Linden, K. G. Phototransformation of selected organophosphorus pesticides: roles of hydroxyl and carbonate radicals. *Water Res.* **2010**, *44*, 3585−3594.
(13) Oturan, N.; Sires, I.; Oturan, M. A.; Brillas, E. Degradation of pesticides in aqueous medium by electro-Fenton and related methods. A review. *J. Environ. Eng. Manage* **2009**, *19*, 235−255.
(14) Chelme-Ayala, P.; El-Din, M. G.; Smith, D. W. Kinetics and mechanism of the degradation of two pesticides in aqueous solutions by ozonation. *Chemosphere* **2010**, *78*, 557−562.
(15) Jaeger, C. D.; Bard, A. J. Spin trapping and electron spin resonance detection of radical intermediates in the photodecomposition of water at TiO_2 particulate systems. *J. Phys. Chem.* **1979**, *83*, 3146−3152.
(16) Evgenidou, E.; Fytianos, K. Photodegradation of triazine herbicides in aqueous solutions and natural waters. *J. Agric. Food Chem.* **2002**, *50*, 6423−6427.
(17) Ying, G.-G.; Williams, B. The degradation of oxadiazon and oxyfluorfen by photolysis. *J. Environ. Sci. Health* **1999**, *B34*, 549−567.
(18) Barcelo, D.; Durand, G.; de Bertrand, N.; Albaiges, J. Determination of aquatic photodegradation products of selected pesticides by gas chromatography-mass spectrometry and liquid chromatography−mass spectrometry. *Sci. Total Environ.* **1993**, *132*, 283−296.
(19) Sanz-Asensio, J.; Plaza-Medina, M.; Martinez-Soria, M. T.; Pérez-Clavijo, M. Study of photodegradation of the pesticide ethiofencarb in aqueous and non-aqueous media, by gas chromatography−mass spectrometry. *J. Chromatogr., A* **1999**, *840*, 235−247.
(20) Bhattacharyya, J.; Banerjee, H.; Bhattacharyya, A. Photodecomposition of an acaricide, fenazaquin, in aqueous alcoholic solution. *J. Agric. Food Chem.* **2003**, *51*, 4013−4016.
(21) Climent, M. J.; Miranda, M. A. Photodegradation of dichlorprop and 2-naphthoxyacetic acid in water. Combined GC−MS and GC−FTIR study. *J. Agric. Food Chem.* **1997**, *45*, 1916−1919.

Received for review July 13, 2010. Revised manuscript received October 17, 2010. Accepted October 22, 2010.